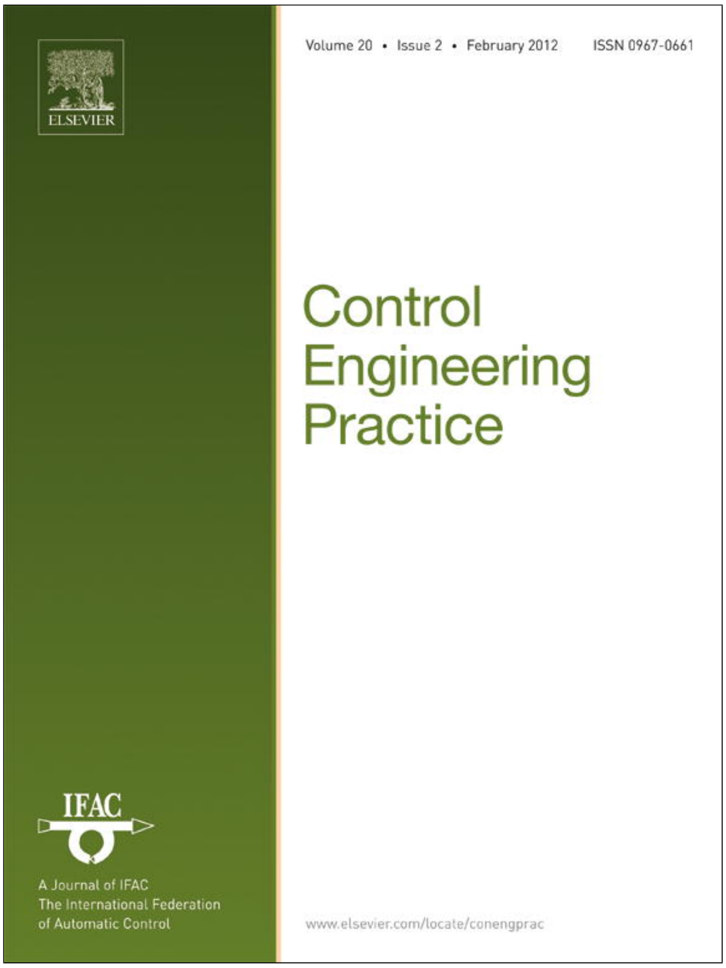
Volume 20 • Issue 2 • February 2012
ISSN 0967-0661
ELSEVIER
Control
Engineering
Practice
IFAC
A Journal of IFAC
The International Federation
of Automatic Control
www.elsevier.com/locate/conengprac

Control Engineering Practice 20 (2012) 111–122

Contents lists available at SciVerse ScienceDirect

Control Engineering Practice

journal homepage: www.elsevier.com/locate/conengprac

Chance-constrained model predictive control for spacecraft rendezvous with disturbance estimation

Francisco Gavilan [a], Rafael Vazquez [a,*], Eduardo F. Camacho [b]

[a] Departamento de Ingeniería Aeroespacial, Escuela Superior de Ingenieros, Universidad de Sevilla, Camino de los Descubrimientos s/n, 41092 Sevilla, Spain
[b] Departamento de Ingeniería de Sistemas y Automática, Escuela Superior de Ingenieros, Universidad de Sevilla, Camino de los Descubrimientos s/n, 41092 Sevilla, Spain

ARTICLE INFO

Article history:
Received 17 December 2010
Accepted 23 September 2011
Available online 29 October 2011

Keywords:
Predictive control
Robust control
Bounded disturbances
Constraint satisfaction problems
Spacecraft autonomy
Space vehicles

ABSTRACT

A robust Model Predictive Controller (MPC) is used to solve the problem of spacecraft rendezvous, using the Hill–Clohessy–Wiltshire model with additive disturbances and line-of-sight constraints. Since a standard (non-robust) MPC is not able to cope with disturbances, a robust MPC is designed using a chance-constrained approach for robust satisfaction of constraints in a probabilistic sense. Disturbances are modeled as Gaussian allowing for an explicit transformation of the probabilistic constraints into simple algebraic constraints. To estimate the distribution parameters a predictor of disturbances is proposed. Both robust and non-robust MPC control laws are compared using the Monte Carlo method, which shows the superiority of the robust MPC.

1. Introduction

Technology enabling simple autonomous spacecraft rendezvous and docking is becoming a growing field as access to space continues to increase. After decades of development, many approaches have been proposed and there have been many experiences, positive and negative; see Woffinden and Geller (2008) for an historical account or Fehse (2003) for the basics. For instance, one of the most recent developments in the field is ESA's Automated Transfer Vehicle (ATV), mainly developed by EADS Astrium, an expendable unmanned spacecraft designed to resupply the International Space Station. ATV has automatic rendezvous capabilities, as demonstrated in its first successful flight in 2008.

The field has become very active in recent years, with an increasingly growing literature; for instance, among many, one can cite Richards, Schouwenaars, How, and Feron (2002), where fuel-optimal trajectories with avoidance constraints are designed using mixed-integer linear programming, Wang, Mokuno, and Hadaegh (2003), which includes autonomous rendezvous and docking capabilities into formation flying satellites, Geller (2006), which uses a linear covariance analysis method to design impulsive maneuvers, or Breger and How (2008), where *safe*, fail-tolerant rendezvous trajectories are planned.

This work approaches the problem of rendezvous of spacecraft using a chance-constrained Model Predictive Control (MPC) with on-line prediction of disturbance statistical properties.

MPC (Camacho & Bordons, 2004) originated in the late seventies and has developed considerably since then. There are many applications of predictive control successfully in use at the current time, not only in the process industry but also in other applications ranging from solar technology (Camacho, Berenguel, & Bordons, 1994) to flight control (Breger & How, 2006). Model Predictive Control is considered to be a mature technique for linear and rather slow systems like the ones usually encountered in the process industry.

The term Model Predictive Control does not designate a specific control strategy but rather an ample range of control methods which make explicit use of a model of the process to obtain the control signal by minimizing an objective function over a finite receding horizon. In MPC the process model is used to predict the future plant outputs, based on past and current values and on the proposed optimal future control actions. These actions are calculated by the optimizer taking into account the cost function (where the fuel cost and the future tracking error are considered) as well as the constraints.

One of the advantages of MPC is that robust control methods can be easily incorporated. In space vehicles, one can find multiple sources of disturbances, such as position or velocity measuring errors, thruster misalignments, or even atmospheric drag; so there is a need to design robust control schemes to deal with these disturbances.

Thus, MPC is very suitable to deal with the problem of spacecraft rendezvous, which is inherently slow and can be very precisely modeled by linear equations (shown in Section 2). The use of robust MPC for rendezvous of spacecraft is not new; for instance Richards and How (2003) analyzes the advantages of robust and non-robust MPC for rendezvous compared with other

* Corresponding author. Fax: +34 954486041.
E-mail addresses: fgavilan@us.es (F. Gavilan), rvazquez1@us.es (R. Vazquez), eduardo@esi.us.es (E.F. Camacho).

0967-0661/$ - see front matter © 2011 Elsevier Ltd. All rights reserved.
doi:10.1016/j.conengprac.2011.09.006

methods. In the work of How and Tillerson (2001) the effect of velocity measurements error during formation flight is taken into account. Sensor errors are modeled, and a robust MPC scheme is proposed that satisfies the constraints for the worst case disturbance, recalculating the trajectory only when the spacecraft get out of a desired error box.

In these works, the key idea is to explicitly take into account system disturbances and uncertainties and to optimize the objective function for the worst case scenario (Camacho & Bordons, 2004). However, for these methods it is necessary to obtain an estimate on the bound of the disturbances. In Richards (2004), several methods for estimation of uncertainty properties are proposed.

This work proposes the use of the so called chance-constrained model predictive control as an alternative to design robust controllers for spacecraft. In this approach, disturbances are incorporated into the problem constraints using a probabilistic formulation. A procedure to transform these probabilistic constraints into algebraic equations is given, and control signals are computed so the constraints are satisfied with a desired probability. Chance-constrained MPC can be found in previous works (mainly for chemical engineering applications), for instance, in Li, Wendt, and Wozny (2000) and Schwarm and Nikolaou (1999) where methods are proposed to deal with linear systems in which uncertainties are present in the step response coefficients of the systems. These authors consider that statistical properties of unknown parameters are acquired off-line.

This work employs an on-line estimator of statistical properties of disturbances together with the chance-constrained formulation of the problem. The advantage of the chance-constrained formulation is that it does not need to know a priori bounds on the size of the disturbances. However, it needs a distribution model for them; a Gaussian model is used which allows for an explicit solution of the probabilistic constraints into algebraic constraints, thus allowing for fast computation of a solution. The parameters of the Gaussian model are inferred from past disturbances using the on-line estimator. To the best of our knowledge, these methods have not been proposed before to solve the problem of spacecraft rendezvous.

The structure of this work is as follows. Section 2 describes the mathematical model for rendezvous spacecraft used for MPC and the constraints of the rendezvous problem. Next, Section 3 follows with a formulation of standard (non-robust) Model Predictive Control suitable for the rendezvous maneuver with continuous thrust. Then the robust chance-constrained MPC is formulated with estimation of disturbance properties. Section 4 shows a Monte Carlo comparison of the robust and non-robust methods. The comparison is also shown for elliptical target orbits, with the discrepancies due to eccentricity considered as a disturbance. Section 5 closes the work with some final remarks.

2. Model of spacecraft rendezvous

There are numerous mathematical models for spacecraft rendezvous; which one should be used depends on the parameters of the scenario. In Carter (1998) a survey of numerous mathematical models for spacecraft rendezvous can be found.

For instance, if the target is orbiting in a *circular* Keplerian orbit, the general equations of the relative movement between an active chaser spacecraft and a passive target vehicle are (see Wie, 1998)

$$\ddot{x} = 2n\dot{y} + n^2(R+x) - \mu\frac{R+x}{[(R+x)^2+y^2+z^2]^{3/2}} + u_x,$$

$$\ddot{y} = -2n\dot{x} + n^2 y - \mu\frac{y}{[(R+x)^2+y^2+z^2]^{3/2}} + u_y,$$

$$\ddot{z} = -\mu\frac{z}{[(R+x)^2+y^2+z^2]^{3/2}} + u_z, \tag{1}$$

where x, y, and z denote the position of the chaser in a local-vertical/local-horizontal (LVLH) frame of reference fixed on the center of gravity of the target vehicle (see Fig. 1), in which x refers to the radial position, y to the in-track position, and z to the cross-track position. The velocity of the chaser in the LVLH frame is given by $\dot{x}$, $\dot{y}$, and $\dot{z}$; and the variables u_x, u_y, and u_z are the inputs (thrust actuation) acting on the chaser vehicle. R is the target orbit radius and $n=\sqrt{\mu/R^3}$ is the angular speed of the target through its orbit (where μ is the gravitation parameter of the Earth, $\mu = 398600.4\ \mathrm{km}^3/\mathrm{s}^2$).

Moreover, if the approaching vehicle is close to the target, Eq. (1) can be linearized around the rendezvous position, leading to the linear Hill–Clohessy–Wiltshire (HCW) equations (introduced in Hill, 1878 and Clohessy & Wiltshire, 1960) which describe with adequate precision the relative position of the spacecraft. The HCW model is the one used throughout this paper, including the possibility of disturbances to allow for unmodeled effects, and the rotation of the target vehicle.

It must be noted that, in many situations, the HCW equations are not accurate. For instance, if the target vehicle is moving in a Keplerian *eccentric* orbit (see Inalhan, Tillerson, & How, 2002) or if some orbital perturbations are taken into account (see for example Humi & Carter, 2008). Section 4 considers simulations with the target orbiting in an eccentric Keplerian trajectory and shows that the control design (based on the HCW equations) still works.

Considering that the control inputs are constant for each sample time interval of duration T, it is possible to derive the following discrete time version of the HCW equations:

$$\mathbf{x}_{k+1} = \mathbf{A}\mathbf{x}_k + \mathbf{B}\mathbf{u}_k + \boldsymbol{\delta}_k, \tag{2}$$

where an unknown vector $\boldsymbol{\delta}_k$ has been added to take into account possible additive disturbances.

In (2), $\mathbf{x}_k$, $\mathbf{u}_k$ and $\boldsymbol{\delta}_k$ denote, respectively, the state, input, and disturbance at time k, where

$$\mathbf{x} = [x\ y\ z\ \dot{x}\ \dot{y}\ \dot{z}]^T, \quad \mathbf{u} = [u_x\ u_y\ u_z]^T, \tag{3}$$

$$\boldsymbol{\delta} = [\delta_x\ \delta_y\ \delta_z\ \delta_{\dot{x}}\ \delta_{\dot{y}}\ \delta_{\dot{z}}]^T, \tag{4}$$

where δ_x, δ_y, δ_z, $\delta_{\dot{x}}$, $\delta_{\dot{y}}$, and $\delta_{\dot{z}}$ represent the disturbances entering the system. Both are referred to the LVLH axes as indicated by their respective subscripts.

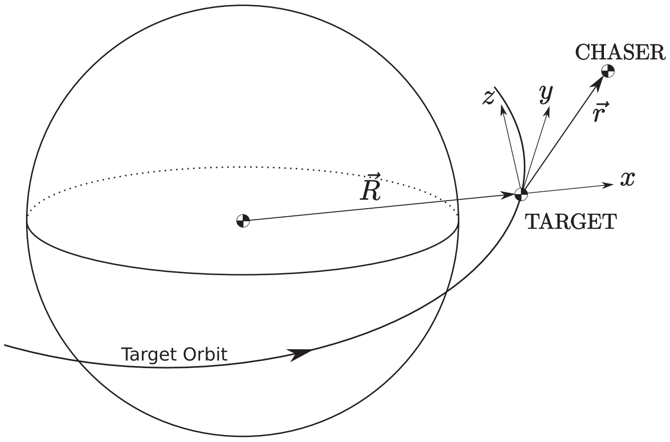

Fig. 1. LVLH frame.

The system (2) will be used for predicting the spacecraft position in the predictive controller formulation (Section 3).

The matrices **A** and **B** appearing in (2) are given by

$$\mathbf{A}=\begin{bmatrix} 4-3C & 0 & 0 & \frac{S}{n} & \frac{2(1-C)}{n} & 0 \\ 6(S-nT) & 1 & 0 & -\frac{2(1-C)}{n} & \frac{4S-3nT}{n} & 0 \\ 0 & 0 & C & 0 & 0 & \frac{S}{n} \\ 3nS & 0 & 0 & C & 2S & 0 \\ -6n(1-C) & 0 & 0 & -2S & 4C-3 & 0 \\ 0 & 0 & -nS & 0 & 0 & C \end{bmatrix}, \tag{5}$$

$$\mathbf{B}=\begin{bmatrix} \frac{1-C}{n^2} & \frac{2nT-2S}{n^2} & 0 \\ \frac{2(S-nT)}{n^2} & -\frac{3T^2}{2}+4\frac{1-C}{n^2} & 0 \\ 0 & 0 & \frac{1-C}{n^2} \\ \frac{S}{n} & 2\frac{1-C}{n} & 0 \\ \frac{2(C-1)}{n} & -3T+4\frac{S}{n} & 0 \\ 0 & 0 & \frac{S}{n} \end{bmatrix}, \tag{6}$$

where $S=\sin nT$ and $C=\cos nT$. The disturbances are unknown, so it is assumed that $\boldsymbol{\delta}_k$ is a random vector, with known distribution but unknown distribution parameters mean $\bar{\boldsymbol{\delta}}$ and covariance $\boldsymbol{\Sigma}$, respectively. These disturbances might arise from errors in the input signals (as thrusters are typically subject to command uncertainties and are never perfectly aligned), or they could also be thought of as unmodeled dynamics (in this case they are not random; however, the randomness assumption is kept for convenience). In Section 4.3 the disturbance model used in simulations is described.

Even though the disturbances are modeled as additive, in Section 4.3 it is shown that the control scheme works for other kind of disturbances such as multiplicative disturbance or modeling errors.

2.1. Constraints on the problem

Two set of constraints are considered in this paper. First, for sensing purposes (see Breger & How, 2008) it is required that the chaser vehicle remains inside a line of sight (LOS) area from the docking point; and second, the amount of thrust that can produce the actuators is bounded.

The LOS area is a region defined to guarantee that the chaser spacecraft is all time visible from the docking point. Thus this area must be defined using a new body fixed frame, since the target can rotate respect to the LVLH axes used in (2), which are fixed to the orbit. Then, once the LOS region is formulated in body axes, a transformation must be used to include these constraints into the rendezvous problem, which is formulated in the LVLH frame.

The target body fixed reference frame is shown in Fig. 2. In this reference system, one can define the LOS region by the equations $y_B \geq c_x(x_B-x_0)$, $y_B \geq -c_x(x_B+x_0)$, $y_B \geq c_z(z_B-z_0)$, $y_B \geq -c_z(z_B+z_0)$ and $y_B \geq 0$ (where x_B, y_B and z_B denote the coordinates in the body fixed frame); as shown in Fig. 2.

The LOS constraint is formulated as $\mathbf{A_L}\mathbf{x}_{\mathbf{B}k} \leq \mathbf{b_L}$, where

$$\mathbf{A_L}=\begin{bmatrix} 0 & -1 & 0 & 0 & 0 & 0 \\ c_x & -1 & 0 & 0 & 0 & 0 \\ -c_x & -1 & 0 & 0 & 0 & 0 \\ 0 & -1 & c_z & 0 & 0 & 0 \\ 0 & -1 & -c_z & 0 & 0 & 0 \end{bmatrix}, \tag{7}$$

$$\mathbf{b_L}=[0 \;\; c_x x_0 \;\; c_x x_0 \;\; c_z z_0 \;\; c_z z_0]^T \tag{8}$$

and $\mathbf{x}_{\mathbf{B}k}$ denotes the state in the body fixed reference frame.

Since these constraints are not defined using the same reference frame than the equation of motion used by the controller (2), a transformation of LOS constraints from body axes to LVLH frame must be done. The transformation of these matrices can be easily computed using projective geometry (see Hartley & Zisserman, 2003).

Using homogeneous coordinates, one can write the equations of a set of n planes as

$$\boldsymbol{\pi}_{(n\times 4)}\tilde{\mathbf{x}}=0, \tag{9}$$

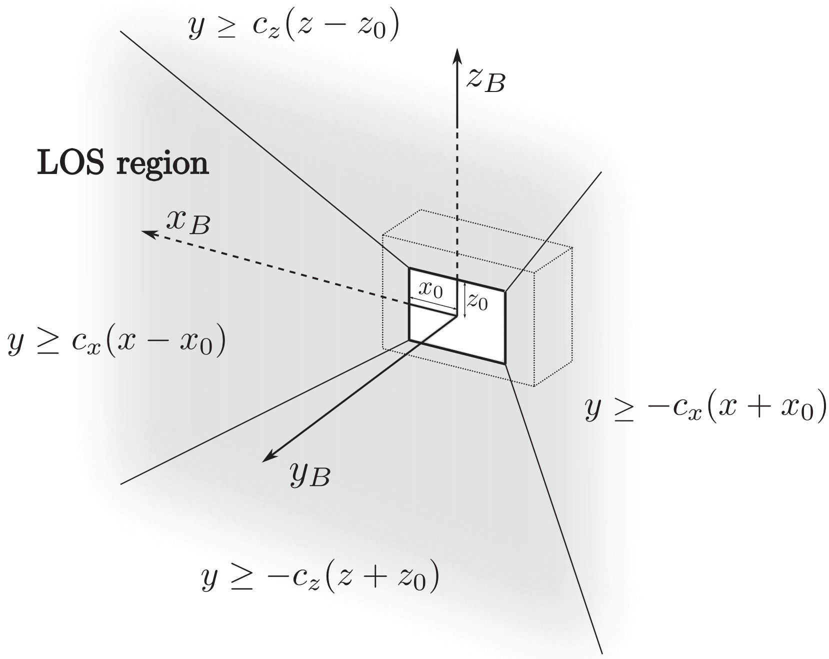

Fig. 2. Line of sight region.

where each row of $\boldsymbol{\pi}$, namely $\boldsymbol{\pi}_i$, defines one plane; and $\tilde{\mathbf{x}}$ is the vector of homogeneous coordinates, that is

$$\tilde{\mathbf{x}} = [x\ \ y\ \ z\ \ 1]^T. \tag{10}$$

It can be proven that under a projective transformation $\tilde{\mathbf{x}} = \mathbf{H}\tilde{\mathbf{x}}'$, a plane transforms as

$$\boldsymbol{\pi}_i' = \boldsymbol{\pi}_i \mathbf{H}, \tag{11}$$

where $\mathbf{H}$ is a transformation matrix in homogeneous coordinates.

In this case, the LOS planes in body axes introduced in (7) and (8) can be defined as:

$$\underbrace{\begin{bmatrix} 0 & -1 & 0 & 0 \\ c_x & -1 & 0 & -c_x x_0 \\ -c_x & -1 & 0 & -c_x x_0 \\ 0 & -1 & c_z & -c_z z_0 \\ 0 & -1 & -c_z & -c_z z_0 \end{bmatrix}}_{\boldsymbol{\pi}_\mathbf{B}} \underbrace{\begin{bmatrix} x_B \\ y_B \\ z_B \\ 1 \end{bmatrix}}_{\tilde{\mathbf{x}}_\mathbf{B}} = 0. \tag{12}$$

The projective transformation between body axes and LVLH frame can be defined as

$$\tilde{\mathbf{x}}_\mathbf{B} = \underbrace{\begin{pmatrix} \mathbf{R}_{3\times 3} & \mathbf{t}_{3\times 1} \\ \mathbf{0}_{1\times 3} & 1 \end{pmatrix}}_{\mathbf{H}} \tilde{\mathbf{x}}_\mathbf{LVLH}, \tag{13}$$

where $\mathbf{R}$ is a rotation matrix from LVLH frame to body axes, and $\mathbf{t}$ is a translation vector which contains the coordinates of center of the LVLH frame respect to the center of the body axes.

Thus, the set of constraint planes in the LVLH frame can be computed as:

$$\boldsymbol{\pi}_\mathbf{LVLH} = \boldsymbol{\pi}_\mathbf{B} \mathbf{H} \tag{14}$$

For instance, if the target spacecraft is rotating around the z_{LVLH} axis with angular velocity Ω, the transformation matrix $\mathbf{H}$ is defined as

$$\mathbf{H} = \begin{bmatrix} C_\Omega & S_\Omega & 0 & 0 \\ -S_\Omega & C_\Omega & 0 & 0 \\ 0 & 0 & 1 & 0 \\ 0 & 0 & 0 & 1 \end{bmatrix}, \tag{15}$$

where $C_\Omega = \cos(\Omega t)$ and $S_\Omega = \sin(\Omega t)$. Thus, the transformed LOS lines are computed as follows:

$$\underbrace{\begin{bmatrix} -S_\Omega & -C_\Omega & 0 & 0 \\ c_x C_\Omega - S_\Omega & -c_x S_\Omega - C_\Omega & 0 & -c_x x_0 \\ -c_x C_\Omega - S_\Omega & c_x S_\Omega - C_\Omega & 0 & -c_x x_0 \\ -S_\Omega & -C_\Omega & c_x & -c_x z_0 \\ -S_\Omega & -C_\Omega & c_z & -c_z z_0 \end{bmatrix}}_{\boldsymbol{\pi}_\mathbf{LVLH}} \begin{bmatrix} x \\ y \\ z \\ 1 \end{bmatrix} = 0, \tag{16}$$

where now x, y and z are the coordinates of the chaser spacecraft in the LVLH frame.

Using these terms, the LOS constraint matrices become:

$$\mathbf{A}_\mathbf{L}' = \begin{bmatrix} -S_\Omega & -C_\Omega & 0 & \\ c_x C_\Omega - S_\Omega & -c_x S_\Omega - C_\Omega & 0 & \\ -c_x C_\Omega - S_\Omega & c_x S_\Omega - C_\Omega & 0 & \boldsymbol{\Theta}_{5\times 3} \\ -S_\Omega & -C_\Omega & c_z & \\ -S_\Omega & -C_\Omega & c_z & \end{bmatrix},$$

$$\mathbf{b}_\mathbf{L}' = [0\ \ c_x x_0\ \ c_x x_0\ \ c_z z_0\ \ c_z z_0]^T, \tag{17}$$

where $\boldsymbol{\Theta}_{5\times 3}$ is a matrix full of zeros, with dimensions 5×3. Notice that in this situation $\mathbf{A}_\mathbf{L}'$ and $\mathbf{b}_\mathbf{L}'$ become time dependent.

Then the LOS constraint in the LVLH frame can be rewritten as:

$$\mathbf{A}_\mathbf{L}' \mathbf{x} \le \mathbf{b}_\mathbf{L}'. \tag{18}$$

Dealing with the control inputs constraints, it is assumed that they are bounded above and below

$$\mathbf{u}_{min} \le \mathbf{u}_k \le \mathbf{u}_{max}, \tag{19}$$

and that $\mathbf{u}_k$ can take any value in the interval, i.e., it is assumed that thruster valves can be opened partially to produce the exact amount of force.

3. Robust MPC formulation

Next a robust MPC scheme is formulated; first some notation is developed to formulate the general problem, and afterwards it is explained how to tackle the disturbances appearing in (2).

3.1. Prediction of the state

The state at time $k+j$, given the state at time k, and the input signals and disturbances from time k to time $k+j-1$, is computed by applying recursively Eq. (2):

$$\mathbf{x}_{k+j} = \mathbf{A}^j \mathbf{x}_k + \sum_{i=0}^{j-1} \mathbf{A}^{j-i-1} \mathbf{B} \mathbf{u}_{k+i} + \sum_{i=0}^{j-1} \mathbf{A}^{j-i-1} \boldsymbol{\delta}_{k+i}. \tag{20}$$

Define now $\mathbf{x}_\mathbf{S}(k)$, $\mathbf{u}_S(k)$, $\boldsymbol{\delta}_\mathbf{S}(k)$ as a stack of $N_p \cdot n_x$ states, $N_p \cdot n_u$ input signals, and $N_p \cdot n_x$ disturbances beginning at time k, where N_p is the prediction horizon, n_x is the number of state variables and n_u is the number of control inputs:

$$\mathbf{x}_\mathbf{S}(k) = \begin{bmatrix} \mathbf{x}_{k+1} \\ \mathbf{x}_{k+2} \\ \vdots \\ \mathbf{x}_{k+N_p} \end{bmatrix}, \quad \mathbf{u}_S(k) = \begin{bmatrix} \mathbf{u}_k \\ \mathbf{u}_{k+1} \\ \vdots \\ \mathbf{u}_{k+N_p-1} \end{bmatrix},$$

$$\boldsymbol{\delta}_\mathbf{S}(k) = \begin{bmatrix} \boldsymbol{\delta}_k \\ \boldsymbol{\delta}_{k+1} \\ \vdots \\ \boldsymbol{\delta}_{k+N_p-1} \end{bmatrix}. \tag{21}$$

Then,

$$\mathbf{x}_\mathbf{S}(k) = \begin{bmatrix} \mathbf{A}\mathbf{x}_k + \mathbf{B}\mathbf{u}_k + \boldsymbol{\delta}_k \\ \mathbf{A}^2 \mathbf{x}_k + \sum_{i=0}^{1} \mathbf{A}^{1-i} (\mathbf{B}\mathbf{u}_{k+i} + \boldsymbol{\delta}_{k+i}) \\ \vdots \\ \mathbf{A}^{N_p} \mathbf{x}_k + \sum_{i=0}^{N_p-1} \mathbf{A}^{N_p-1-i} (\mathbf{B}\mathbf{u}_{k+i} \boldsymbol{\delta}_{k+i}) \end{bmatrix}, \tag{22}$$

which can be written as

$$\mathbf{x}_\mathbf{S}(k) = \mathbf{F}\mathbf{x}_k + \mathbf{G}_\mathbf{u} \mathbf{u}_S(k) + \mathbf{G}_\delta \boldsymbol{\delta}_\mathbf{S}, \tag{23}$$

where $\mathbf{G}_\mathbf{u}$ and $\mathbf{G}_\delta$ are block lower triangular matrix with its non-null elements defined by $(\mathbf{G}_\mathbf{u})_{ij} = \mathbf{A}^{i-j}\mathbf{B}$ and $(\mathbf{G}_\delta)_{ij} = \mathbf{A}^{i-j}$ (with $i \ge j$), and the matrix $\mathbf{F}$ is defined as:

$$\mathbf{F} = \begin{bmatrix} \mathbf{A} \\ \mathbf{A}^2 \\ \vdots \\ \mathbf{A}^{N_p} \end{bmatrix}. \tag{24}$$

Note that it is assumed that the control logic has perfect knowledge of the state vector $\mathbf{x}_k$.

3.2. Objective function

Taking mathematical expectation, define $\hat{\mathbf{x}}_{k+j|k} = E[\mathbf{x}_{k+j}]$, the expected value of $\mathbf{x}_{k+j}$ given $\mathbf{x}_k$. Similarly define $\hat{x}_S(k+j|k) = E[\mathbf{x}_S(k+j)]$. For the MPC formulation the following cost function is used:

$$J(k)=\sum_{i=1}^{N_p}[\hat{\mathbf{x}}_{k+i|k}^T\mathbf{R}(k+i)\hat{\mathbf{x}}_{k+i|k}]+\sum_{i=1}^{N_p}[\mathbf{u}_{k+i-1}^T\mathbf{Id}_{3\times3}\mathbf{u}_{k+i-1}], \quad (25)$$

where the matrix $\mathbf{R}(k)$ is defined as

$$\mathbf{R}(k)=\gamma h(k-k_a)\begin{bmatrix}\mathbf{Id}_{3\times3} & \mathbf{\Theta}_{3\times3}\\ \mathbf{\Theta}_{3\times3} & \mathbf{\Theta}_{3\times3}\end{bmatrix}. \quad (26)$$

In (26), h is the step function, k_a is the desired arrival time for docking, γ a large positive number, and $\mathbf{Id}_{3\times3}$, $\mathbf{\Theta}_{3\times3}$ are, respectively, the identity matrix and a matrix full of zeros, both of order 3 by 3.

The reason for choosing (26) is that it is desired to arrive at the origin at time k_a (and *remain* there) and at the same time minimize the control effort.

Remark 1. The relative position during the maneuver is not important as long as constraints are satisfied and docking is reached on time.

Using (23), and since $E[\boldsymbol{\delta}(k+i)]=\overline{\boldsymbol{\delta}}$, Eq. (25) can be rewritten as:

$$J(k)=(\mathbf{G_u}\mathbf{u}_S(k)+\mathbf{F}\mathbf{x}_k+\mathbf{G}_\delta\overline{\boldsymbol{\delta}}_\mathbf{S})^T\mathbf{R_S}(\mathbf{G_u}\mathbf{u}_S(k)+\mathbf{F}\mathbf{x}_k+\mathbf{G}_\delta\overline{\boldsymbol{\delta}}_\mathbf{S})+\mathbf{u}_S^T\mathbf{Q}_S\mathbf{u}_S, \quad (27)$$

where $\overline{\boldsymbol{\delta}}_\mathbf{S}$ is a stack vector with $\overline{\boldsymbol{\delta}}$ repeated N_p times, $\mathbf{Q}_S=\mathbf{Id}_{3N_p\times3N_p}$ and $\mathbf{R_S}$ is a block diagonal matrix defined by:

$$\mathbf{R_S}=\begin{bmatrix}\mathbf{R}(k+1) & & \\ & \ddots & \\ & & \mathbf{R}(k+N_p)\end{bmatrix}. \quad (28)$$

Using the notation above developed with the LOS constraints formulated in Section 2.1, the constraints equations for the state can be rewritten as:

$$\mathbf{A_c}\mathbf{x_S}\le\mathbf{b_c}, \quad (29)$$

where $\mathbf{A_c}$ and $\mathbf{b_c}$ are given by:

$$\mathbf{A_c}=\begin{bmatrix}\mathbf{A}'_\mathbf{L}(k+1) & & \\ & \ddots & \\ & & \mathbf{A}'_\mathbf{L}(k+N_p)\end{bmatrix},$$

$$\mathbf{b_c}=[\mathbf{b}'_\mathbf{L}(k+1)\ \cdots\ \mathbf{b}'_\mathbf{L}(k+N_p)]^T. \quad (30)$$

Using Eq. (23), one can reformulate the LOS constraints as constraints for the control signals in the following way:

$$\mathbf{A_c}\mathbf{G_u}\mathbf{u}_S\le\mathbf{b_c}-\mathbf{A_c}\mathbf{F}\mathbf{x}_k-\mathbf{A_c}\mathbf{G}_\delta\boldsymbol{\delta}_\mathbf{S}, \quad (31)$$

and similarly it is possible to write (19) as:

$$\tilde{\mathbf{u}}_{min}\le\mathbf{u_S}\le\tilde{\mathbf{u}}_{max}, \quad (32)$$

being $\tilde{\mathbf{u}}_{min}$ and $\tilde{\mathbf{u}}_{max}$ stacks of $N_p\times n_u$ minimum and maximum bounds of the control input.

3.3. Computation of control input

To compute the control input at time k, one seeks the control signal that minimizes the cost function over the prediction horizon, satisfying at the same time the constraints:

$$\begin{aligned}&\min_{\mathbf{u}_S} J(\mathbf{x}_k,\mathbf{u}_S,\overline{\boldsymbol{\delta}}_\mathbf{S}),\\ &\text{s.t.}\quad \mathbf{A_c}\mathbf{G_u}\mathbf{u}_S\le\mathbf{b_c}-\mathbf{A_c}\mathbf{F}\mathbf{x}_k-\mathbf{A_c}\mathbf{G}_\delta\boldsymbol{\delta}_\mathbf{S}\quad\forall\boldsymbol{\delta}_\mathbf{S},\\ &\tilde{\mathbf{u}}_{min}\le\mathbf{u_S}\le\tilde{\mathbf{u}}_{max}.\end{aligned} \quad (33)$$

Since the cost function is quadratic and the constraints are linear, if the future disturbance $\boldsymbol{\delta}$ is perfectly known (for example, in the undisturbed case) then (33) can be solved; the control $\mathbf{u}_k$ is set to the first three components of $\mathbf{u_S}$, and the computation is repeated for every time step.

However, if the disturbances are not known but rather their mean and variance are known, it is necessary to modify (33), as it is explained next.

3.4. Robust satisfaction of constraints

To eliminate the disturbances from (31), a bound of the term $-\mathbf{A_c}\mathbf{G}_\delta\boldsymbol{\delta}_\mathbf{S}$ must be found to enforce the satisfaction of constraints in presence of disturbances. Two procedures are given, depending on which disturbance properties are available.

Assume first that some bounds for the disturbances are known, i.e., $\boldsymbol{\delta}$ has the property that $(\delta_x)_{\min}\le\delta_x\le(\delta_x)_{\max}$ and similarly for the rest of the components of δ. Those bounds are summarized as $\mathbf{A}_\delta\boldsymbol{\delta}_\mathbf{S}\le\mathbf{c}_\delta$. Hence, it is assumed that the region defined by this constraint is enclosed by a polytope. Then, it is possible to eliminate the disturbances from (31) by bounding the term $-\mathbf{A_c}\mathbf{G}_\delta\boldsymbol{\delta}_\mathbf{S}$. This would give

$$\mathbf{A_c}\mathbf{G_u}\mathbf{u}_S\le\mathbf{b}_c-\mathbf{A_c}\mathbf{F}\mathbf{x}_k-\mathbf{A_c}\mathbf{G}_\delta\boldsymbol{\delta}_\mathbf{S}\le\mathbf{b}_c-\mathbf{A_c}\mathbf{F}\mathbf{x}_k+\mathbf{b}_\delta(k), \quad (34)$$

where $\mathbf{b}_\delta(k)$ is column vector, whose i-th term $(\mathbf{b}_\delta(k))_i$ is given by

$$\begin{aligned}&(\mathbf{b}_\delta(k))_i=\min_{\boldsymbol{\delta}_S} a_i\boldsymbol{\delta}_\mathbf{S},\\ &\text{s.t.}\quad \mathbf{A}_\delta\boldsymbol{\delta}_\mathbf{S}\le\mathbf{c}_\delta,\end{aligned} \quad (35)$$

where a_i is the i-th *row* of the matrix $-\mathbf{A_c}\mathbf{G}_\delta$. Since the function to minimize is linear and the feasible region is enclosed by a polytope, this minimization can be rapidly solved.

Eq. (34) represents the constraints computed for the *worst-case* disturbances. Hence, enforcing (34) the constraints (29) are robustly satisfied, i.e., satisfied for *any possible disturbance*.

However, if the disturbance bounds are not precisely known, but the disturbance is modeled as a random vector, the inequality $\mathbf{b}_\delta(k)\le-\mathbf{A_c}\mathbf{G}_\delta\boldsymbol{\delta}_\mathbf{S}$ is made to be satisfied with a certain probability. This probability should be near one, thus guaranteeing that the inequality is satisfied for *almost all* disturbances.

Assuming that the disturbances are normally distributed ($\boldsymbol{\delta}\sim N_6(\overline{\boldsymbol{\delta}},\mathbf{\Sigma})$), and that their mean ($\overline{\boldsymbol{\delta}}$) and covariance matrix ($\mathbf{\Sigma}=\mathbf{\Sigma}^T>0$) are known, it is possible to write (see Rencher, 1998)

$$\delta\sim N_6(\overline{\boldsymbol{\delta}},\mathbf{\Sigma})\Rightarrow(\boldsymbol{\delta}-\overline{\boldsymbol{\delta}})^T\mathbf{\Sigma}^{-1}(\boldsymbol{\delta}-\overline{\boldsymbol{\delta}})\sim\chi^2(6), \quad (36)$$

where $\chi^2(6)$ is a chi-square probability distribution with six degrees of freedom.

Assuming that the statistical properties of the disturbances are time-invariant, Eq. (36) is valid for the disturbances at all times $k+j$ for $j=0,\ldots,N_p-1$:

$$\begin{aligned}&(\boldsymbol{\delta}_{k+j}-\overline{\boldsymbol{\delta}})^T\mathbf{\Sigma}^{-1}(\boldsymbol{\delta}_{k+j}-\overline{\boldsymbol{\delta}})\sim\chi^2(6),\\ &j=0,\ldots,N_p-1.\end{aligned} \quad (37)$$

Hence, finding α from the equation:

$$\mathrm{P}(\chi^2(6)\le\alpha)=p, \quad (38)$$

it is guaranteed with probability p that

$$(\boldsymbol{\delta}_{k+j}-\overline{\boldsymbol{\delta}})^T\mathbf{\Sigma}^{-1}(\boldsymbol{\delta}_{k+j}-\overline{\boldsymbol{\delta}})\le\alpha. \quad (39)$$

Thus, p is a parameter of the control design and should be close to unity.

Then, dividing the inequality by α, $\mathbf{b}_\delta(k)$ can be found by solving the following minimization problem for each row i of $\mathbf{A_c}\mathbf{G}_\delta$.

$$\begin{aligned}&(\mathbf{b}_\delta(k))_i=\min_{\boldsymbol{\delta}_S} a_i\boldsymbol{\delta}_\mathbf{S},\\ &\text{s.t.}\quad(\boldsymbol{\delta}_{k+j}-\overline{\boldsymbol{\delta}})^T(\alpha\mathbf{\Sigma})^{-1}(\boldsymbol{\delta}_{k+j}-\overline{\boldsymbol{\delta}})\le1,\\ &j=0,\ldots,N_p-1,\end{aligned} \quad (40)$$

where a_i and $(\mathbf{b}_\delta(k))_i$ are the i-th *row* of the matrix $-\mathbf{A_c G_\delta}$ and the vector $\mathbf{b}_\delta(k)$, respectively.

Now, breaking down the stack vector $\boldsymbol{\delta}_\mathbf{S}$ into each of its components $\boldsymbol{\delta}_k$ up to $\boldsymbol{\delta}_{k+N_p-1}$, it is possible to write $a_i\boldsymbol{\delta}_\mathbf{S} = \sum_{j=0}^{N_p-1} a_{ij}\boldsymbol{\delta}_{k+j}$. Thus, the minimization problem can be written as:

$$(\mathbf{b}_\delta(k))_i = \min_{\boldsymbol{\delta}_{k+j}} \sum_{j=0}^{N_p-1} a_{ij}\boldsymbol{\delta}_{k+j},$$
$$\text{s.t.} \quad (\boldsymbol{\delta}_{k+j}-\overline{\boldsymbol{\delta}})^T(\alpha\boldsymbol{\Sigma})^{-1}(\boldsymbol{\delta}_{k+j}-\overline{\boldsymbol{\delta}}) \le 1,$$
$$j=0,\ldots,N_p-1. \tag{41}$$

Defining $\mathbf{z}(j) = \mathbf{H}^{\frac{1}{2}}(\boldsymbol{\delta}_{k+j}-\overline{\boldsymbol{\delta}})$, where $\mathbf{H} = (\alpha\boldsymbol{\Sigma})^{-1}$ (being $\mathbf{H}=\mathbf{H}^T>0$), it is possible to write (41) as:

$$(\mathbf{b}_\delta)_i = \min_{\mathbf{z}(j)} \sum_{j=0}^{N_p-1} (a_{ij}\mathbf{H}^{-1/2}\mathbf{z}(j) + a_{ij}\overline{\boldsymbol{\delta}}),$$
$$\text{s.t.} \quad \mathbf{z}(j)^T\mathbf{z}(j) \le 1, \quad j=0,\ldots,N_p-1, \tag{42}$$

which can be rewritten as

$$(\mathbf{b}_\delta)_i = \sum_{j=0}^{N_p-1}\left(\min_{\mathbf{z}(j)}(a_{ij}\mathbf{H}^{-1/2}\mathbf{z}(j)) + a_{ij}\overline{\boldsymbol{\delta}}\right),$$
$$\text{s.t.} \quad \mathbf{z}(j)^T\mathbf{z}(j) \le 1,$$
$$j=0,\ldots,N_p-1. \tag{43}$$

Problem (43) can be explicitly solved independently for each j via the Lagrange formalism, yielding the minimum at

$$\mathbf{z}^*(j) = -\frac{\mathbf{H}^{-1/2}a_{ij}^T}{\sqrt{a_{ij}\mathbf{H}^{-1}a_{ij}^T}}. \tag{44}$$

Substituting into (43) the rows of the vector $\mathbf{b}_\delta(k)$ are

$$(\mathbf{b}_\delta(k))_i = \sum_{j=0}^{N_p-1}\left(-\sqrt{a_{ij}\mathbf{H}^{-1}a_{ij}^T} + a_{ij}\overline{\boldsymbol{\delta}}\right). \tag{45}$$

Once the vector $\mathbf{b}_\delta(k)$ is calculated (using Eq. (35) or (45)), the control input at time k is now computed from

$$\min_{\mathbf{u}_S} J(\mathbf{x}_k,\mathbf{u}_S,\overline{\boldsymbol{\delta}}_\mathbf{S}),$$
$$\text{s.t.} \quad \mathbf{A_c G_u u}_S \le \mathbf{b_c} - \mathbf{A_c F x}_k + \mathbf{b}_\delta(k),$$
$$\tilde{\mathbf{u}}_{min} \le \mathbf{u_S} \le \tilde{\mathbf{u}}_{max}, \tag{46}$$

where now everything is known except for the control inputs to be computed.

In simulations, the probabilistic method is used to compute the robust MPC control.

3.5. Disturbance estimation algorithm

The robust satisfaction of constraints presented in Section 3.4 requires knowledge of disturbance statistical properties. However, it is often the case that such properties are completely unknown and have to be obtained on-line.

To do so, it is assumed that the disturbances are normally distributed with mean $\overline{\boldsymbol{\delta}}$ and covariance matrix $\boldsymbol{\Sigma}$, i.e., $\delta \sim N_6(\overline{\boldsymbol{\delta}},\boldsymbol{\Sigma})$.

At each time k, $\overline{\boldsymbol{\delta}}$ and $\boldsymbol{\Sigma}$ are estimated taking into account all *past* disturbances, which can be computed a posteriori as

$$\boldsymbol{\delta}_i = \mathbf{x}_{i+1} - \mathbf{A}\mathbf{x}_i - \mathbf{B}\mathbf{u}_i, \tag{47}$$

for $i=1,\ldots,k-1$.

Then $\hat{\boldsymbol{\delta}}_k$ and $\hat{\boldsymbol{\Sigma}}_k$, the estimates of $\overline{\boldsymbol{\delta}}$ and variance $\boldsymbol{\Sigma}$ at time k, based on disturbances up to time $k-1$, are given by

$$\hat{\boldsymbol{\delta}}_k = \frac{\sum_{i=0}^{k-1} \mathrm{e}^{-\lambda(k-i)}\boldsymbol{\delta}_i}{\sum_{i=0}^{k-1}\mathrm{e}^{-\lambda(k-i)}}, \tag{48}$$

$$\hat{\boldsymbol{\Sigma}}_k = \frac{\sum_{i=0}^{k-1} \mathrm{e}^{-\lambda(k-i)}(\boldsymbol{\delta}_i-\hat{\boldsymbol{\delta}}_k)(\boldsymbol{\delta}_i-\hat{\boldsymbol{\delta}}_k)^T}{\sum_{i=0}^{k-1}\mathrm{e}^{-\lambda(k-i)}}, \tag{49}$$

where $\lambda > 0$ is a *forgetting factor*. Even though it has been assumed that the disturbances are just a random variable, this would help accommodate the case in which they are a *random process*, i.e., their statistical properties change with time.

Define $\gamma_k = \sum_{i=0}^{k-1}\mathrm{e}^{-\lambda(k-i)}$. Using the sum of a geometric progression,

$$\gamma_k = \frac{\mathrm{e}^{-\lambda}(1-\mathrm{e}^{-\lambda k})}{1-\mathrm{e}^{-\lambda}}. \tag{50}$$

Then, it is possible to define recursive formulas for (48) and (49) as follows:

$$\hat{\boldsymbol{\delta}}_k = \frac{\mathrm{e}^{-\lambda}}{\gamma_k}(\gamma_{k-1}\hat{\boldsymbol{\delta}}_{k-1} + \boldsymbol{\delta}_{k-1}), \tag{51}$$

$$\hat{\boldsymbol{\Sigma}}_k = \frac{\mathrm{e}^{-\lambda}}{\gamma_k}(\gamma_{k-1}\hat{\boldsymbol{\Sigma}}_{k-1} + (\boldsymbol{\delta}_{k-1}-\hat{\boldsymbol{\delta}}_k)(\boldsymbol{\delta}_{k-1}-\hat{\boldsymbol{\delta}}_k)^T), \tag{52}$$

with $\hat{\boldsymbol{\delta}}_0 = 0$, $\hat{\boldsymbol{\Sigma}}_0 = 0$.

These formulas allow to save memory, only needing to store the last estimate of the mean and covariance.

Once the mean and covariance are estimated, the procedure outlined in Section 3.4 can be used.

4. Simulation results

4.1. Rendezvous model

It is important to remark that although the controller shown in Section 3 is designed using the linear HCW model (2), in simulations the general nonlinear model of spacecraft rendezvous (1) has been considered.

Dealing with the model parameters, it has been considered that the case of a target spacecraft flying in a circular orbit at 500 km of altitude, which means that $R_0 = 6878$ km and $n = 1.1068\times 10^{-3}$ rad/s.

Concerning the constraints, the maximum and minimum amount of acceleration that can provide the chaser's actuators are $u_{max} = 10^{-3}$ m/s^2 and $u_{min} = -10^{-3}$ m/s^2, respectively (all the actuators have the same values). The LOS area is estated with the parameters: $x_0 = z_0 = 1.5$ m and $c_x = c_z = 1$ (see Fig. 2).

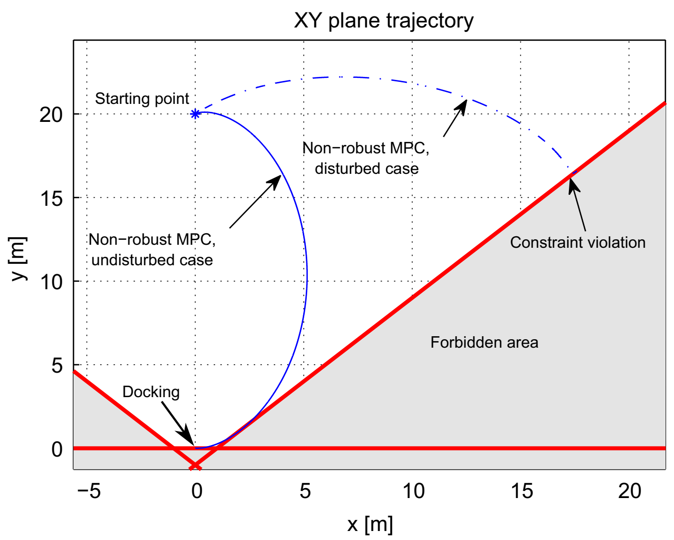

Fig. 3. Non-robust MPC without disturbances (solid line) and with disturbances (dashed line). For clarity, only the *XY* plane is shown.

In addition, in some simulations it has been considered that the target vehicle has an eccentric orbit. In these cases, the motion of each vehicle is simulated separately using the general equation for a Keplerian orbit (which can be found in Wie, 1998), and then differentiating both trajectories to obtain the relative position.

4.2. Disturbances model

When designing the control laws, it was considered that the commanded forces were equal to $\mathbf{u}_{real} = [u_x\ u_y\ u_z]^T$, which are the *real* forces applied to the spacecraft. To include disturbances, $\mathbf{u}_{real}$ is modeled not as being the exact control signal commanded by the controller, but rather as

$$\mathbf{u}_{real} = \mathbf{T}(\boldsymbol{\delta\theta})(\mathbf{u}+\boldsymbol{\delta}_1), \tag{53}$$

where $\mathbf{u}$ is the *commanded* output computed by the control laws, $\boldsymbol{\delta}_1$ is a random variables, and $\mathbf{T}(\boldsymbol{\delta\theta})$ is a rotation matrix where $\boldsymbol{\delta\theta}$ is a vector of small, random angles modeling imperfect alignment.

Hence in this case the disturbance $\boldsymbol{\delta} = \mathbf{B}((\mathbf{T}(\boldsymbol{\delta\theta}) - \mathbf{Id})\mathbf{u} + \mathbf{T}(\boldsymbol{\delta\theta})\boldsymbol{\delta}_1)$, which is not strictly an additive disturbance. The matrix $\mathbf{B}$ is defined in Eq. (6).

These disturbances model several physical aspects. First, the attitude control of the chaser is not perfect, so one can expect some alignment errors; those are modeled by $\mathbf{T}(\boldsymbol{\delta\theta})$. It can be noted that the disturbance attitude angles may not have zero mean value, since some bias in the sensors or actuators can exist and lead to a steady state error. On the other hand, with $\boldsymbol{\delta}_1$ one can model thrust disturbances. Notice that it might have nonzero mean value, introducing some bias in the thrust level.

Finally, it must be noted that in several simulations, an eccentric orbit of the target spacecraft have been considered, so equations (1) are no longer valid. The new equations of movement are given in reference Inalhan et al. (2002). Since the circular equations (1) are similar to the eccentric equations (at least for moderate values of eccentricity) the difference between the models can be thought of as unmodeled dynamics.

4.3. Simulation results

4.3.1. Robust vs non-robust controller

Next the results obtained by the non-robust controller (33) are shown, where the disturbances are just ignored. In Fig. 3, two scenarios are considered: one ideal case in which disturbances do not exist (solid line) and another more realistic situation in which thrusters disturbances and misalignments errors are present. The non-robust controller achieves perfect rendezvous for the nominal case satisfying the constraints, whereas in the perturbed case the controller violates the constraints and is not able to reach the target.

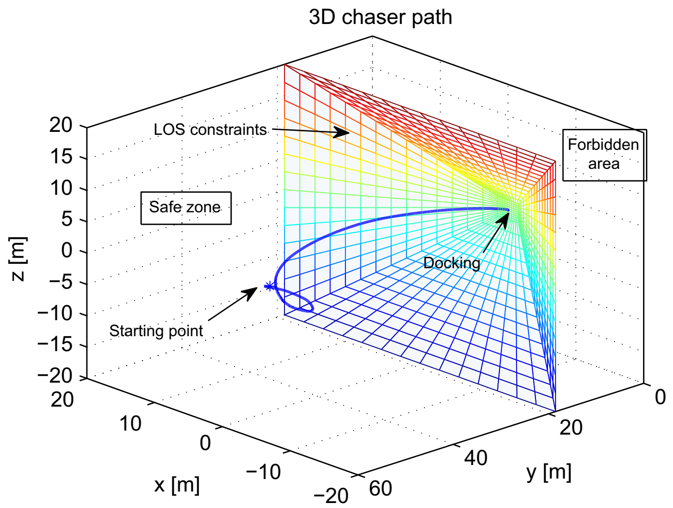

Fig. 4. Path followed by the chaser spacecraft ($\boldsymbol{\delta}_1 : \overline{\boldsymbol{\delta}} = [0.2592\ \ 0.8065\ \ -0.0533] \times 10^{-4}$, $\sqrt{\Sigma_{ii}} = 1 \times 10^{-5}$; $\boldsymbol{\delta\theta} : \overline{\delta}_i = 0.0436$, $\sqrt{\Sigma_{ii}} = 0.0436$). Controller parameters are $N_p = 60$, $\gamma = 1000$, $k_a = 60$, $p = 0.95$, $\lambda = 0.23$.

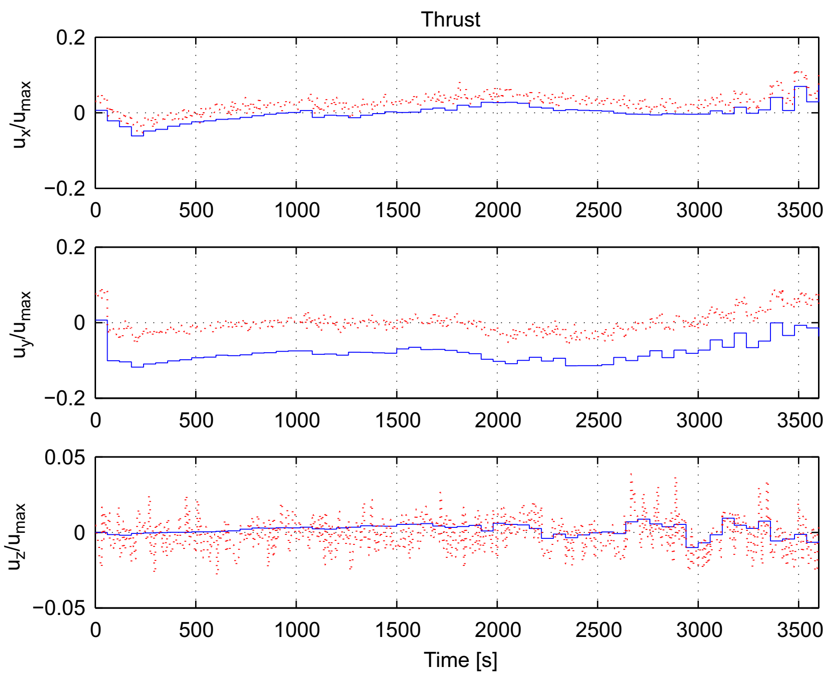

Fig. 5. Control signals ($\boldsymbol{\delta}_1 :\ \overline{\boldsymbol{\delta}} = [0.2592\ \ 0.8065\ \ -0.0533] \times 10^{-4}$, $\sqrt{\Sigma_{ii}} = 1 \times 10^{-5}$; $\boldsymbol{\delta\theta} : \overline{\delta}_i = 0.0436$, $\sqrt{\Sigma_{ii}} = 0.0436$). Controller parameters are $N_p = 60$, $\gamma = 1000$, $k_a = 60$, $p = 0.95$, $\lambda = 0.23$. The solid and dotted lines represent the commanded control signals ($\mathbf{u}$) and the real control applied ($\mathbf{u}_{real}$), respectively. Notice that u_{max} for all the actuators was defined as $u_{max} = 10^{-3}$ m/s^2.

Introducing now the robust MPC controller designed in Section 3.4, a rendezvous maneuver in a disturbed environment is shown in Fig. 4, where, it can be seen that now the chaser spacecraft's path is maintained inside the safe zone. In Fig. 5, the control signals computed by the robust MPC controller (solid lines) and the real forces applied to the spacecraft (dotted lines) are presented. Notice the disturbances in the real control signals applied, which have severe bias and large typical deviation.

The trajectory followed by the chaser spacecraft is also shown in Fig. 6. It can be seen that the controller is not only able to make the spacecraft follow a safe path, but also guarantees that the target is reached on time.

Since the disturbances introduced in the model are random variables with normal distribution of probability (see Section 4.2), a Monte Carlo analysis is conducted to get more confidence on the controller design. A number of 1220 simulations have been done for both robust and non-robust controllers, using same the parameters and disturbance distribution for both cases. The selected parameters were $N_p=60$, $\gamma=1000$, $k_a=60$, $p=0.975$, $\lambda=0.1$ and $T=40$ s. Regarding the disturbances, since the mean of the bias in the thrust force ($\overline{\boldsymbol{\delta}}_1$) has a strong influence in the simulation result, its value was selected for each simulation in the interval $\overline{\delta}_i \in [-0.05u_{max}, 0.05u_{max}]$ m/s, with constant probability. The standard deviation for $\boldsymbol{\delta}_1$ was $\sqrt{\Sigma_{ii}}=0.01u_{max}$. The statistical properties of the misalignment disturbance vector $\boldsymbol{\delta\theta}$ were set to the same values as shown in Fig. 5.

The result of the analysis is summarized in Table 1, where the advantages of the robust MPC can be seen. In 100% of the scenarios simulated, the robust controller was able to achieve rendezvous, guiding the chaser spacecraft to a docking position less than 20 cm (d denotes the distance to the target at the arrival time). The non-robust controller only could achieve the rendezvous in the 40.9% of the cases, reaching docking positions farther than the robust one.

In addition, it can be seen that the robust controller is not only able to achieve the rendezvous with more guarantees but it also can do the maneuver with less cost. Fig. 7 plots the mission cost

Table 1
Results of a simulation batch of 1220 cases for both robust and non-robust controllers. d is the distance the relative distance at the desired arrival time.

Performance indicator	Non-robust MPC (%)	Robust MPC (%)
Constraint violations	59	0
$d \le 0.2$ m	19	100
0.2 m $\le d \le 0.5$ m	22	0
0.5 m $\le d$	0	0
Mean cost (m/s) of successful missions	0.2444	0.2039

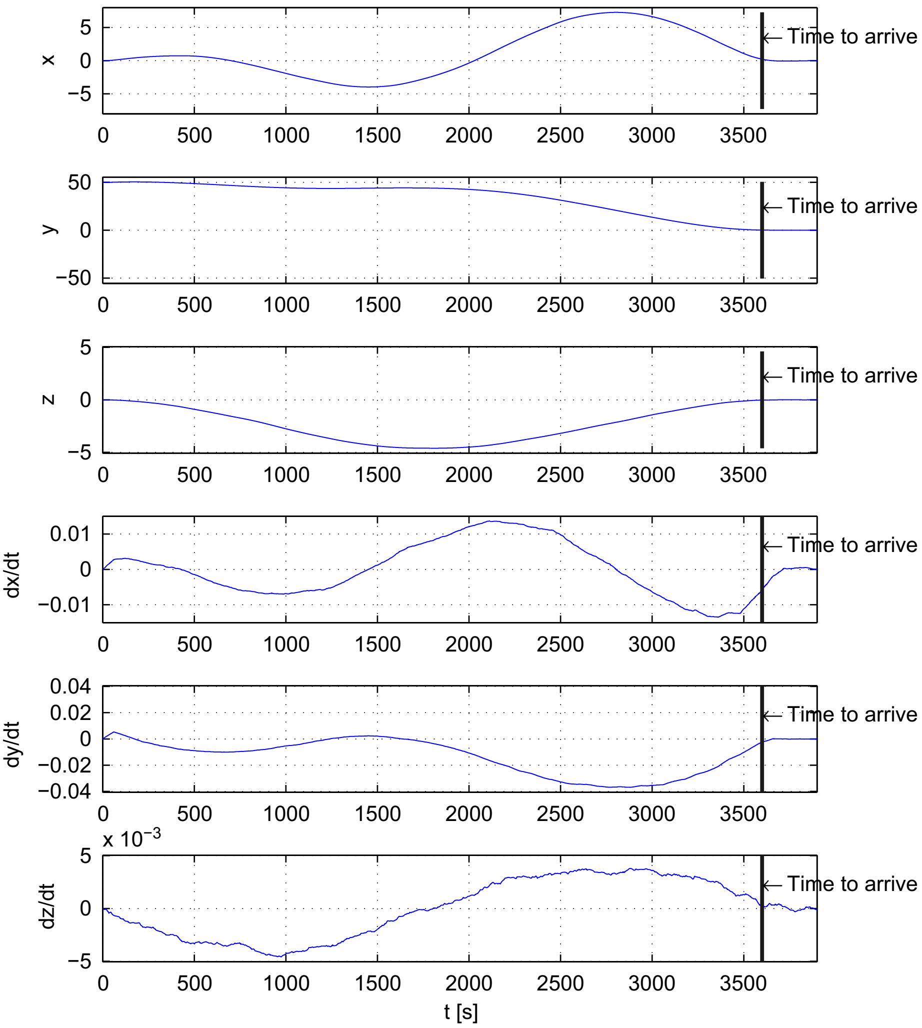

Fig. 6. Time evolution of the system states ($\boldsymbol{\delta}_1$: $\overline{\boldsymbol{\delta}}=[0.2592\ \ 0.8065\ \ -0.0533]\times 10^{-4}$, $\sqrt{\Sigma_{ii}}=0.5\times 10^{-5}$; $\boldsymbol{\delta\theta}$: $\overline{\delta}_i=0.0436$, $\sqrt{\Sigma_{ii}}=0.0436$). Controller parameters are $N_p=60$, $\gamma=1000$, $k_a=60$, $p=0.95$, $\lambda=0.23$.

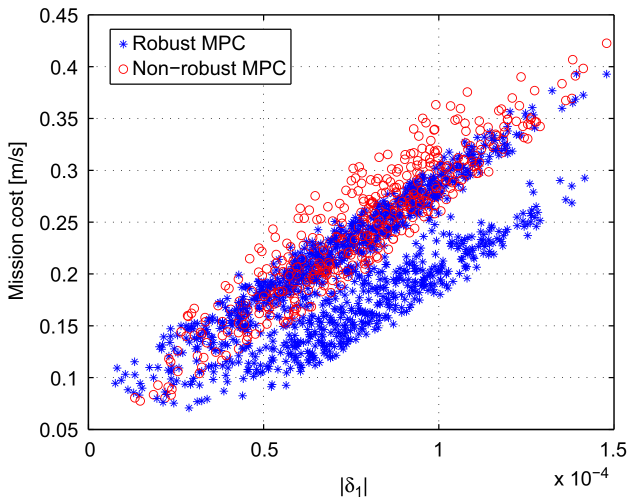

Fig. 7. Mission cost plotted against the L_1-norm of the mean of the disturbance vector $\overline{\boldsymbol{\delta}}_{\mathbf{1}}$.

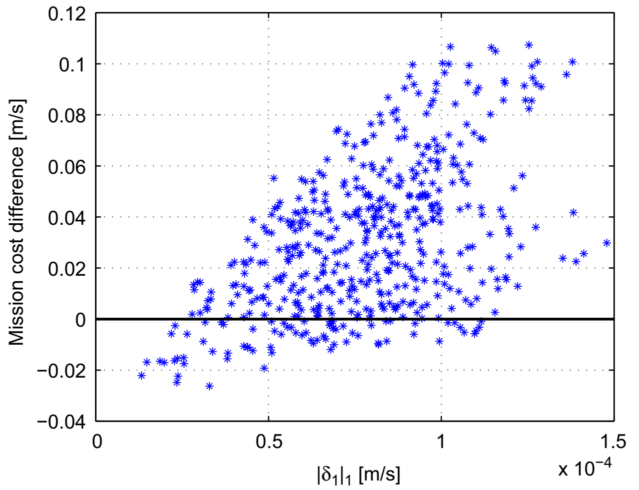

Fig. 8. Increment of the non-robust controller mission cost with respect to the robust one (in m/s), plotted against the L_1-norm of the mean of the disturbance vector $\overline{\boldsymbol{\delta}}_{\mathbf{1}}$. Only successful missions are compared.

obtained for each simulation, against the L_1-norm of the mean disturbance vector $\overline{\boldsymbol{\delta}}_{\mathbf{1}}$. Notice that only successful missions are depicted in the figure and that the number of points corresponding to the non-robust MPC is significantly smaller than the number corresponding to the robust MPC, where all missions were successful. For both controllers, the cost seems to increase with $|\overline{\boldsymbol{\delta}}_{\mathbf{1}}|_1$, but in most cases, the robust controller can achieve the rendezvous with less cost than the non-robust one.

This fact is appreciated in Fig. 8 where is plotted the increment in the mission cost of the non-robust controller respect to the robust one, in the cases when both controllers can achieve rendezvous without constraints violations. It can be found that using the non-robust controller implies a 15% of cost increment.

4.3.2. *Eccentric orbit*

Unmodeled dynamics due by eccentricity (e) in the target orbit are considered next. Several values of the target eccentricity are tested for both robust and non-robust controllers, without considering thruster and misalignments disturbances.

The controller parameters are set to the same values as in the Monte Carlo analysis. The results obtained can be seen in Figs. 9 and 10 (notice that only the *XY*-plane is represented for more simplicity). It is shown that even in the absence of thruster or misalignments disturbances, the presence of an eccentric orbit causes the non-robust controller to violate the constraints (see Fig. 9), while the robust controller is able to achieve the rendezvous without constraint violations (Fig. 10).

4.3.3. *Rotating target*

In the previous simulations, the target spacecraft has a fixed attitude in the LVLH frame (this means that the target spacecraft has a rotation respect to an inertial reference system with orbital frequency n), however, it might be possible to find situations in which the target spacecrafts is not fixed to this frame.

For instance, let consider the case in which it is desired that the target spacecraft is pointing to a fixed direction (for example, to a fixed star). Then it must have some angular velocity respect to the LVLH frame, since these axes are rotating with angular velocity $\Omega_{LVLH} = n\mathbf{k}_{LVLH}$ respect to an inertial reference frame.

Then, to maintain the target attitude fixed to an inertial frame, it must have an angular velocity $\Omega_{target} = -n\mathbf{k}_{LVLH}$. Thus, the LOS constraint (which are defined in a body fixed reference frame)

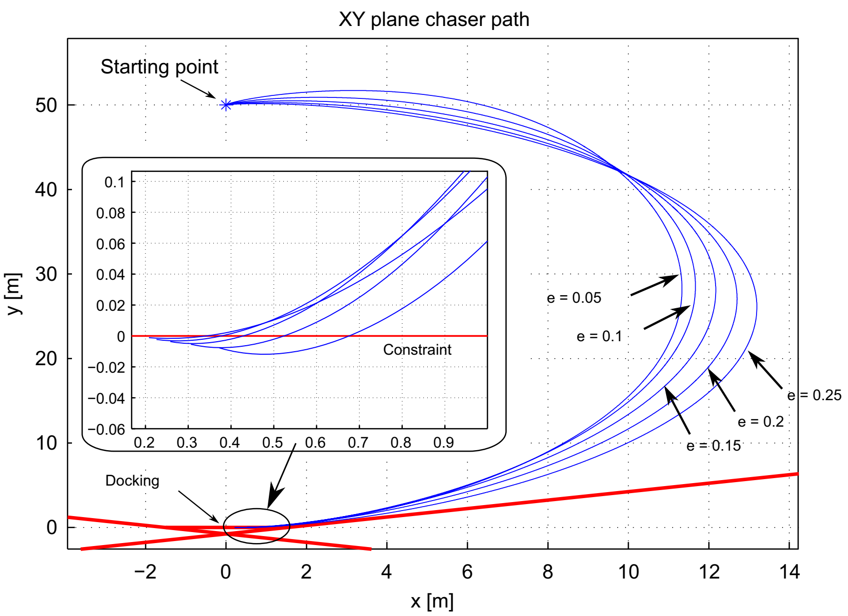

Fig. 9. Non-robust MPC with unmodeled dynamics. Controller parameters are N_p=60, γ = 1000, k_a=60 and T = 45 s.

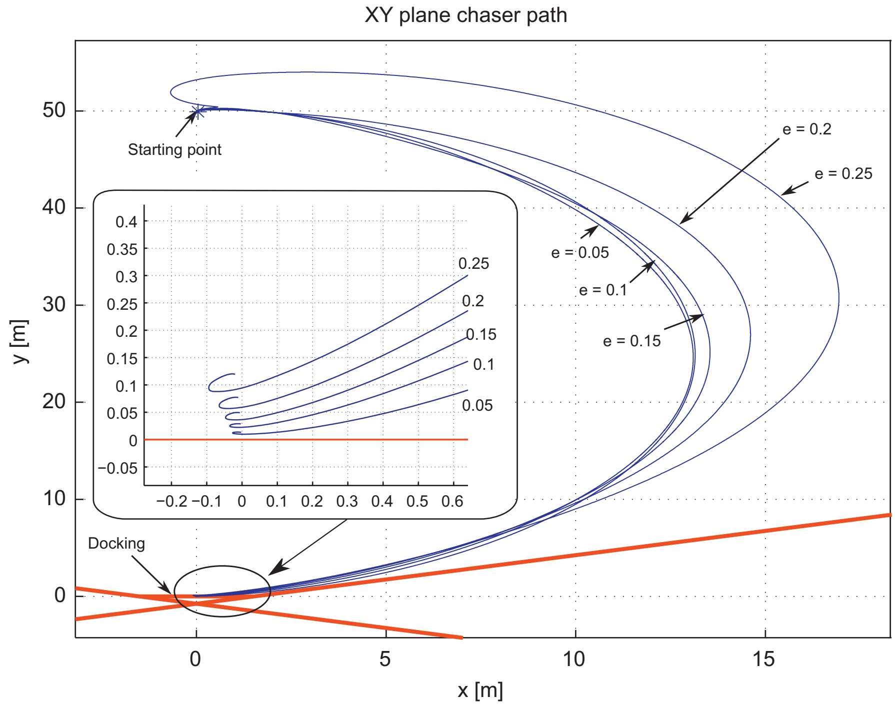

Fig. 10. Robust MPC with unmodeled dynamics. Controller parameters are N_p=60, $\gamma = 1000$, k_a=60, p=0.99, $\lambda = 0.23$ and $T = 45$ s.

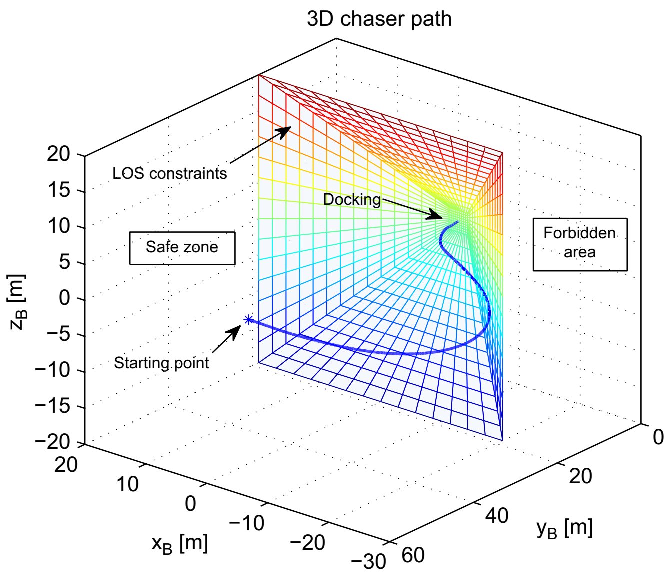

Fig. 11. Path followed by the chaser spacecraft when the target has an angular velocity $\Omega_{target} = -n\mathbf{k}_{LVLH}$ ($\boldsymbol{\delta}_1$: $\bar{\boldsymbol{\delta}}$=[0.2592 0.8065 −0.0533] $\times 10^{-4}$, $\sqrt{\Sigma_{ii}} = 1 \times 10^{-5}$; $\boldsymbol{\delta\theta}$: $\bar{\delta}_i = 0.0436$, $\sqrt{\Sigma_{ii}} = 0.0436$). Controller parameters are N_p=60, $\gamma = 1000$, k_a=60, p=0.95, $\lambda = 0.23$. The axis displayed in the figure are fixed on the rotating target spacecraft.

must be transformed into the LVLH frame using the procedure given in Section 2.1, being the transformation matrix:

$$\mathbf{H} = \begin{bmatrix} \cos(nt) & -\sin(nt) & 0 & 0 \\ \sin(nt) & \cos(nt) & 0 & 0 \\ 0 & 0 & 1 & 0 \\ 0 & 0 & 0 & 1 \end{bmatrix}. \tag{54}$$

Notice that these constraints are time dependent.

In Fig. 11 is shown the rendezvous maneuver with the target spacecraft rotating at $\Omega_{target} = -1.1068 \times 10^{-3}\mathbf{k}_{LVLH}$. It can be seen that the chaser is able to follow the LOS-zone movement, and as shown in Fig. 13 (which depicts the time evolution of the system states) it achieves rendezvous at the desired time. Additionally, the applied control signals during the maneuver are shown in Fig. 12.

5. Concluding remarks

Autonomous rendezvous and proximity operations are a vital element to enable a more operationally responsive space. These procedures are rather complex and technologically demanding; in particular, increasing autonomy presents a serious challenge from the point of view of control theory. Thus, there is an emerging necessity to develop easy-to-implement rendezvous control laws able to comply with severe safety restrictions and cope with disturbances and unmodeled dynamics, while at the same time optimizing fuel consumption. This work described a robust Model Predictive Controller that solves the rendezvous problem using the Hill–Clohessy–Wiltshire model with disturbances and line-of-sight constraints. The performance of the controller is demonstrated in simulations. It is first shown that standard Model Predictive Control is not able to cope with disturbances, justifying the necessity to formulate a robust controller. It is shown that using a Gaussian probabilistic model for the disturbances and a disturbance estimator to compute the estimated disturbance mean and covariance, it is possible to formulate a robust Model Predictive Control that robustly satisfies the problem constraint without significantly increasing the control law computation time. Even though simple models (Hill–Clohessy–Wiltshire rendezvous model, additive Gaussian disturbances, thrusters capable of a continuous range of thrust) were used in the control law formulation, simulation results demonstrate the controller effectiveness for more complex situations, such as multiplicative disturbances or unmodeled dynamics (due to eccentricity of the orbit of the target spacecraft). In conclusion, the robust model predictive controller described provides an implementable, fuel-efficient, and computationally feasible control algorithm for

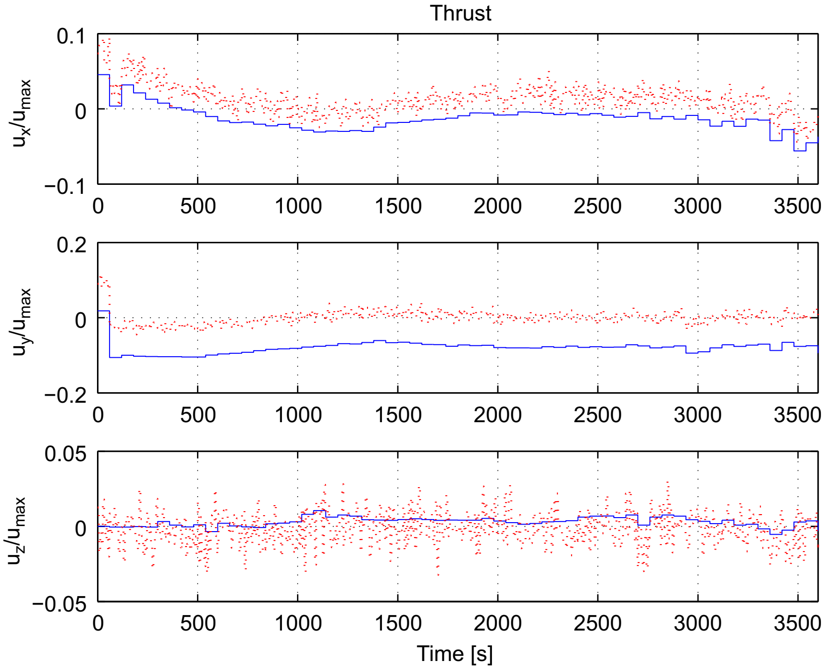

Fig. 12. Control signals ($\boldsymbol{\delta}_1 : \overline{\boldsymbol{\delta}} = [0.2592\ \ 0.8065\ \ -0.0533] \times 10^{-4}$, $\sqrt{\Sigma_{ii}} = 1 \times 10^{-5}$; $\boldsymbol{\delta\theta} : \overline{\delta}_i = 0.0436$, $\sqrt{\Sigma_{ii}} = 0.0436$). Controller parameters are N_p=60, $\gamma = 1000$, k_a=60, p=0.95, $\lambda = 0.23$. The solid and dotted lines represent the commanded control signals ($\mathbf{u}$) and the real control applied ($\mathbf{u}_{real}$), respectively. Notice that u_{max} for all the actuators was defined as $u_{max} = 10^{-3}$ m/s^2.

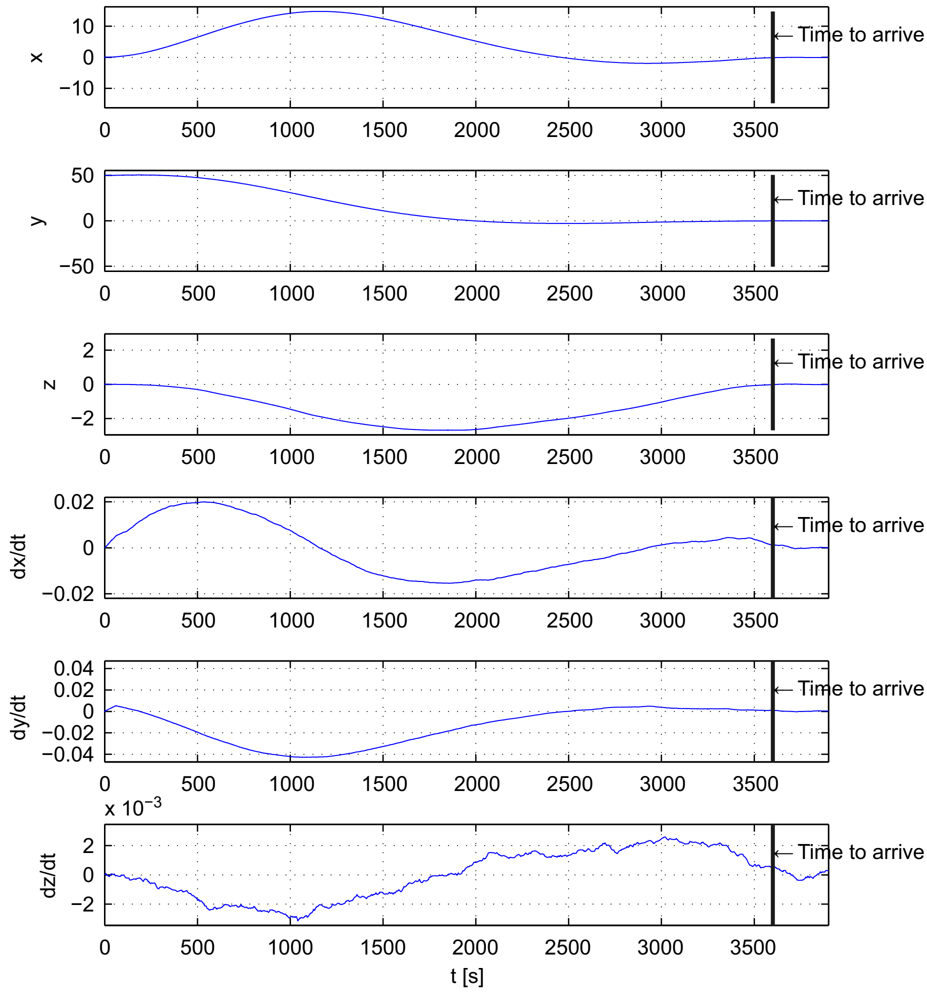

Fig. 13. Time evolution of the system states ($\boldsymbol{\delta}_1 : \overline{\boldsymbol{\delta}} = [0.2592\ \ 0.8065\ \ -0.0533] \times 10^{-4}$, $\sqrt{\Sigma_{ii}} = 1 \times 10^{-5}$; $\boldsymbol{\delta\theta} : \overline{\delta}_i = 0.0436$, $\sqrt{\Sigma_{ii}} = 0.0436$). Controller parameters are N_p=60, $\gamma = 1000$, k_a=60, p=0.95, $\lambda = 0.23$.

spacecraft rendezvous procedures in the presence of model uncertainties and disturbances.

Acknowledgments

The authors thank Teodoro Alamo for pointing out the probabilistic method of Section 3.4.

The authors would also like to gratefully acknowledge MICINN and Junta de Andalucia for funding part of this work under grants DPI2008-05818 and P07-TEP-02720.

References

Breger, L., & How, J. P. (2006). Nonlinear model predictive control technique for unmanned air vehicles. *Journal of Guidance, Control and Dynamics*, *29*(5), 1179–1188.
Breger, L., & How, J. P. (2008). Safe trajectories for autonomous rendezvous of spacecraft. *Journal of Guidance, Control and Dynamics*, *31*(5), 1478–1489.
Camacho, E., Berenguel, M., & Bordons, C. (1994). Adaptive generalized predictive control of a distributed collector field. *IEEE Transactions on Control Systems Technology*, *2*, 462–468.
Camacho, E. F., & Bordons, C. (2004). *Model predictive control* (2nd ed.). Springer-Verlag (pp. 131–205).
Carter, T. E. (1998). State transition matrices for terminal rendezvous studies: Brief survey and new example. *Journal of Guidance, Control and Dynamics*, *21*(1), 148–155.
Clohessy, W. H., & Wiltshire, R. S. (1960). Terminal guidance systems for satellite rendezvous. *Journal of the Aerospace Sciences*, *27*(9), 653–658.
Fehse, W. (2003). *Automated rendezvous and docking of spacecraft* (1st ed.). Cambridge, UK: Cambridge University Press (pp. 171–215).
Geller, D. (2006). Linear covariance techniques for orbital rendezvous analysis and autonomous onboard mission planning. *Journal of Guidance, Control and Dynamics*, *29*(6), 1404–1414.
Hartley, R., & Zisserman, A. (2003). *Multiple view geometry in computer vision* (2nd ed.). Cambridge, UK: Cambridge University Press (pp. 26–36).
Hill, G. (1878). Researches in lunar theory. *American Journal of Mathematics*, *1*(3), 5–26. 129–147, 245–260.
How, J., & Tillerson, M. (2001). Analysis of the impact of sensor noise on formation flying control. in: *American Control Conference*, vol. 5.
Humi, M., & Carter, T. (2008). Orbits and relative motion in the gravitational field of an oblate body. *Journal of Guidance, Control and Dynamics*, *31*(3), 522–532.
Inalhan, G., Tillerson, M., & How, J. P. (2002). Relative dynamics and control of spacecraft formations in eccentric orbits. *Journal of Guidance, Control and Dynamics*, *25*(1), 48–59.
Li, P., Wendt, M., & Wozny, G. (2000). Robust model predictive control under chance constraints. *Computers and Chemical Engineering*, *24*(2–7), 829–834.
Rencher, A. C. (1998). *Multivariate statistical inference and applications* (1st ed.). New York: Wiley (pp. 40–42).
Richards, A., Schouwenaars, T., How, J. P., & Feron, E. (2002). Spacecraft trajectory planning with avoidance constraints using mixed-integer linear programming. *Journal of Guidance, Control, and Dynamics*, *25*(4), 755–764.
Richards, A. G. (2004). *Robust constrained model predictive control*. Ph.D. Thesis. Cambridge, MA: Massachusetts Institute of Technology, (pp. 27–77).
Richards, A. G., & How, J. (2003). *Performance evaluation of rendezvous using model predictive control*. AIAA Paper 2003-5507.
Schwarm, A., & Nikolaou, M. (1999). Chance-constrained model predictive control. *AIChE Journal*, *45*(8), 1743–1752.
Wang, P., Mokuno, M., & Hadaegh, F. (2003). *Formation flying of multiple spacecraft with automatic rendezvous and docking capability*. AIAA Paper 2003-5363.
Wie, B. (1998). *Space vehicle dynamics and control*. AIAA Education Series.
Woffinden, D. C., & Geller, D. K. (2008). Navigating the road to autonomous orbital rendezvous. *Journal of Spacecraft and Rockets*, *44*(4), 898–909.